J. Fetal Med. (September 2019) 6:127–132
https://doi.org/10.1007/s40556-019-00219-5

ORIGINAL ARTICLE

Fetal MRI to Assess an Aberrant Artery in Bronchopulmonary Sequestration: The Utility of a Single-Shot Turbo Spin Echo Sequence

Hidekazu Aoki[1] · Osamu Miyazaki[1] · Reiko Okamoto[1] · Yoshiyuki Tsutsumi[1] · Mikiko Miyasaka[1] · Haruhiko Sago[2] · Yutaka Kanamori[3] · Takako Yoshioka[4] · Shunsuke Nosaka[1]

Received: 19 July 2019 / Accepted: 9 September 2019 / Published online: 17 September 2019

Abstract Detecting an aberrant artery is the key to diagnosing bronchopulmonary sequestration (BPS) on fetal MRI. Few reports describe the best sequence to use for this purpose. We compared visualization of an aberrant artery in BPS on fetal MRI using single-shot turbo spin echo (SSTSE) and balanced steady state free precession (b-SSFP) sequences. We retrospectively reviewed the fetal MRI of 27 fetuses in which BPS was diagnosed prenatally (2003–2016). From these we selected 15 fetuses with the pathological diagnosis of BPS made postnatally at operation. All fetuses were examined in 1.5 T MRI units using SSTSE and b-SSFP sequences (mean gestational age: 28.4 ± 3.4 weeks). Two pediatric radiologists compared visualization of the aberrant artery using the two sequences. The presence of an aberrant artery was confirmed by postnatal contrast-enhanced CT. The influence of arterial diameter and background heterogeneity of the lung on the diagnostic power was also evaluated. All 15 fetuses clearly showed the aberrant artery on the SSTSE sequence. Conversely, the aberrant arteries detected on the SSTSE sequence were absent in the b-SSFP sequences of eight fetuses, and the other seven fetuses showed ambiguous visualization compared with the SSTSE sequence. Arterial diameter and background heterogeneity did not affect the diagnostic power in either sequence. The SSTSE sequence was superior to the b-SSFP sequence for clear visualization of the aberrant artery in BPS, regardless of the arterial diameter and background heterogeneity.

Keywords Bronchopulmonary sequestration · Aberrant artery · Single-shot turbo spin echo sequence · Steady state free precession sequence · MRI · Fetus

Introduction

Bronchopulmonary sequestration (BPS) consists of anomalous lung tissue with systemic arterial supply (an aberrant artery)—one of the congenital bronchopulmonary malformations. BPS accounts for approximately 10–20% of all fetal pulmonary masses and is the second most common congenital lung malformation after congenital pulmonary airway malformation (CPAM) [1, 2]. BPS is further classified into extralobar sequestration (ELS), with its own pleura and no communication to the bronchial tree, and intralobar sequestration (ILS). ILS does not have separate pleura and may communicate with the bronchial tree [3, 4]. The aberrant artery most commonly originates from the lower thoracic aorta, the abdominal aorta or one of its branches [5, 6]. BPS typically appears as a well-defined, homogeneous solid mass in the lower hemithorax on fetal MRI, similar to microcystic CPAM. However, BPS occasionally presents as a heterogeneous mass with a cystic component termed a "hybrid lesion" (BPS and CPAM)'; the CPAM is generally macrocystic [1, 2]. The key to differentiating between CPAM and BPS or hybrid lesions

✉ Hidekazu Aoki
hdkz0706@gmail.com

[1] Department of Radiology, National Center for Child Health and Development, 2-10-1, Okura, Setagaya-ku, Tokyo 157-8535, Japan

[2] Center for Maternal-Fetal, Neonatal and Reproductive Medicine, National Center for Child Health and Development, Tokyo, Japan

[3] Division of Surgery, Department of Surgical Specialties, National Center for Child Health and Development, Tokyo, Japan

[4] Department of Pathology, National Center for Child Health and Development, Tokyo, Japan

is detection of an aberrant artery. If there is an aberrant artery, CPAM is excluded.

The diagnosis of BPS can be established by detecting the aberrant artery on prenatal color Doppler ultrasound. However, fetal MRI can be also informative through the acquisition of additional information about anatomical relationships and occult complications, owing to its high contrast resolution. It is also less affected by maternal obesity, oligohydramnios, and fetal position [7]. Detection of an aberrant artery on fetal MRI is known to be one of the best supportive techniques for confirming the diagnosis. However, previous literature and textbooks have not yet described which sequence might be best for evaluation of the aberrant artery in BPS.

A fast imaging technique is essential for fetal MRI to decrease motion artifacts, and therefore single-shot turbo spin echo (SSTSE) and balanced-steady state free precession (b-SSFP) sequences are widely used [2, 8]. An SSTSE sequence involves fast imaging based on single slice acquisition, the standard technique for evaluation on T2-weighted images. In contrast, the b-SSFP sequence uses gradient echo acquisition for fast imaging: all slices are acquired simultaneously. It is widely used for cardiac and abdominal vessels imaging and for whole-body fetal screening. This is because it is thought to be safer for the fetus due to the lower radiofrequency (RF) absorption than occurs with an SSTSE sequence [9].

The aim of our study is to compare visualization of the aberrant artery in BPS by fetal MRI using SSTSE and b-SSFP sequences.

Materials and Methods

This retrospective study was approved by the institutional review board of the study site, who waived informed consent.

Fetus Selection

We retrospectively reviewed all 27 fetuses who were prenatally diagnosed with BPS at our institution between 2003 and 2016 using fetal MRI. Of these, 15 fetuses (28.4 ± 3.4 weeks' gestation (mean ± SD), range 23–34 weeks, Table 1) were selected as they had a pathological diagnosis of BPS and underwent contrast-enhanced CT and surgery postnatally. The other 12 fetuses were excluded for the following reasons: eight cases were observed without surgery, three cases were lost to follow-up, and one case was accompanied by severe fetal hydrops and died soon after birth (contrast-enhanced CT was not performed).

Image Acquisition

All fetuses were examined using 1.5 T MRI units (fetuses #1–9: Gyroscan Intera, Philips Medical Systems, Best, The Netherlands; fetuses #10–15: MAGNETOM Aera, Siemens Healthineers, Erlangen, Germany). Slice thickness and slice gap were as follows: 3.5 mm, 0.35 mm (SSTSE, Gyroscan Intera), 4.5 mm, − 2 mm (b-SSFP, Gyroscan Intera), and 5 mm, 0.5 mm (SSTSE and b-SSFP, MAGNETOM Aera). Our routine protocol for fetal lung disease consists of two planes (axial and coronal) on SSTSE sequences, three planes (axial, coronal, and sagittal) on b-SSFP sequences, and the sagittal plane on a T1-weighted, fast low-angle shot sequence. Two pediatric radiologists (H.A., O.M.; 12 years and 29 years of experience respectively) reviewed and reconfirmed the visualization of aberrant arteries in all planes of the SSTSE and b-SSFP sequences by comparing the fetal MRI and postnatal contrast-enhanced CT images. The MRI diagnosis of an aberrant artery was established if a linear structure was present, communicating with the aorta and leading towards the sequestration, and this was consistent with the CT findings. The initial contrast-enhanced CT was performed at 7.3 ± 12.9 days old (mean ± SD) with a range of 1–54 days. For fetuses #1–8 we used an 8-detector row Light-Speed Ultra scanner (GE Healthcare, Milwaukee, WI); and for fetuses #9–15, a 64-detector row Discovery CT750 HD scanner (GE Healthcare, Milwaukee, WI), with CTDI vol 2.4 ± 1.0 mGy (mean ± SD, 16 cm phantom); range 1.0–4.6 mGy).

Perspectives in Assessment

Visualization of the aberrant artery on each of the SSTSE and b-SSFP sequences was assessed respectively from three perspectives:

1. The diagnostic power of the images—visualization of the aberrant artery on SSTSE and b-SSFP sequences

The visualization of the aberrant artery was rated using a three-point Likert scale (good, fair, or poor) on both SSTSE and b-SSFP sequences as follows: good, 3 (well identified); fair, 2 (ambiguously identified); and poor, 1 (not identified). This rating scale was formulated based on discussion between the two radiologists. If different findings were seen on different scan planes in the same patient, the best result was adopted based on consensus following discussion. We statistically evaluated the summed scores between the images on SSTSE and b-SSFP using a paired *t* test.

2. The relationship between the diagnostic power of the images and arterial diameter

Table 1 Summary of fetuses (gender, gestational weeks, and final diagnosis of BPS at operation), comparison of arterial diameter and visualization on b-SSFP, comparison of pathology and diagnostic power

Visualization of aberrant arteries on SSTSE and b-SSFP sequences (Result 1)						Arterial diameter and diagnostic power on b-SSFP (Result 2)		Pathology and diagnostic power (Result 3)			
Fetus	Gender	Gestational weeks	Final diagnosis of BPS at operation	Likert scale		DIAMETER (MM)		SSTSE		b-SSFP	
				SSTSE	b-SSFP	Fair	Poor	BPS	Hybrid	BPS	Hybrid
1	M	33	Rt. ELS	3	1		1.4	3		1	
2	M	29	Lt. ILS	3	2	2.2			3		2
3	M	34	Lt. ELS	3	2	1.2		3		2	
4	F	27	Lt. ILS	3	1		2.3		3		1
5	F	26	Rt. ILS	3	2	2.4			3		2
6	F	23	Rt. ILS	3	1		2	3		1	
7	M	27	Lt. ELS	3	2	1.7			3		2
8	F	23	Rt. ILS	3	1		1.9		3		1
9	M	24	Lt. ILS	3	1		3		3		1
10	F	30	Rt. ILS	3	2	3			3		2
11	F	31	Lt. ELS	3	2	2.8		3		2	
12	M	26	Rt. ILS	3	2	3.1			3		2
13	F	30	Rt. ILS	3	1		2.9		3		1
14	M	31	Rt. ILS	3	1		3.7		3		1
15	M	32	Lt. ELS	3	1		3.5	3		1	
Mean				3	1.47	2.3	2.6	3	3	1.4	1.5
				$P < 0.01$ (0.0007)		$P = 0.27$				$P = 0.37$	

SSTSE single-shot turbo spin echo, *b-SSFP* balanced steady state free precession, *M* male, *F* female, *Rt* right, *Lt* left, *ELS* extralobar sequestration, *ILS* intralobar sequestration, *BPS* bronchopulmonary sequestration

3 = good (well identified), 2 = fair (ambiguously identified), 1 = poor (not identified)

The maximum diameter of the aberrant artery (region of origin) was measured on postnatal axial contrast-enhanced CT using a measuring tool from the picture archiving and communication system (PACS; Centricity PACS RA1000 Workstation, GE Healthcare, Milwaukee, WI). The relationship between the mean arterial diameter and the three-point Likert scale (good, fair, and poor respectively) was evaluated statistically using a Fisher's exact test.

3. Diagnostic power of imaging in the BPS and hybrid lesion

BPS and hybrid lesions were distinguished based on pathological findings. If cystic or emphysematous changes were pathologically identified, the lesion was classified as a hybrid lesion. The relationship between the pathological groups (BPS or hybrid lesion) and the three-point Likert scale (good, fair, and poor respectively) was evaluated statistically using a Fisher's exact test.

All analyses were performed using Microsoft Excel (Microsoft Corporation, Redmond, WA). A *P* value of less than 0.05 was regarded as statistically significant.

Results

All three sets of results are summarized in Table 1.

1. The diagnostic power of the images—visualization of the aberrant artery on SSTSE and b-SSFP sequences

All 15 aberrant arteries were well visualized on SSTSE sequences ('good' in all fetuses, #1–15, Figs. 1, 2). Conversely, there were those rated as absent ('poor', n = 8 (47%), fetuses #1, 4, 6, 8, 9, and 13–15, Fig. 1) and ambiguous ('fair', n = 7 (53%), fetuses #2, 3, 5, 7, and 10–12, Fig. 2) on b-SSFP sequences. There was no case where visualization of an aberrant artery was good on

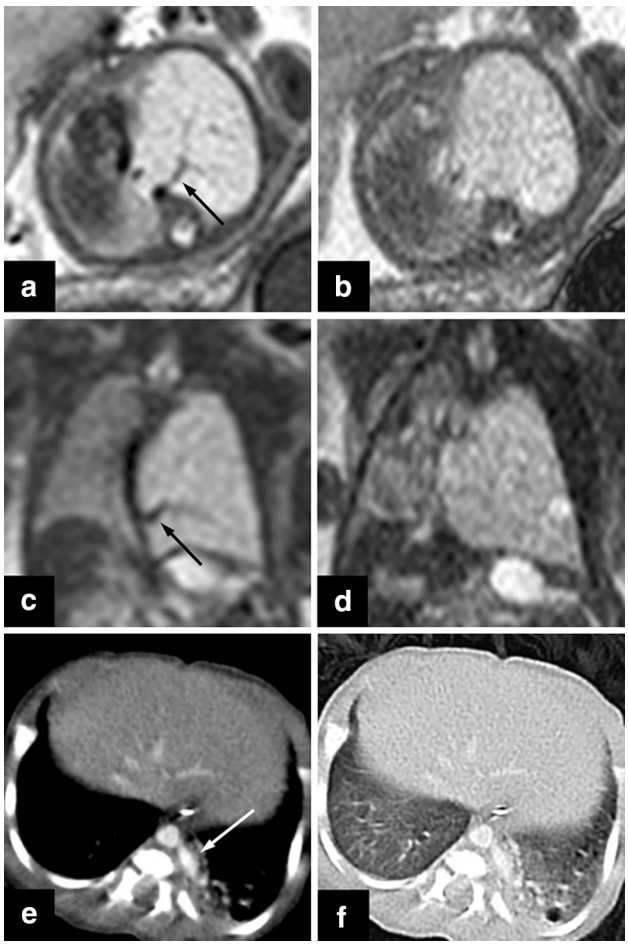

Fig. 1 ILS in the left lower lobe (typical images representing "good" on SSTSE and "poor" on b-SSFP sequence, fetus #9). **a–d** Fetal MRI at 24 weeks' gestation (**a** SSTSE axial plane, **b** b-SSFP axial plane, **c** SSTSE coronal plane, **d** b-SSFP coronal plane). Aberrant artery (arrow) is well identified on the SSTSE sequence (**a**, **c**), conversely it is absent on the b-SSFP sequence (**b**, **d**). Contrast-enhanced CT at the age of 2 days after birth reveals the aberrant artery (arrow) which shows a similar appearance to the fetal MRI, though the sequestration is smaller than in the fetal MRI (**e**, **f**)

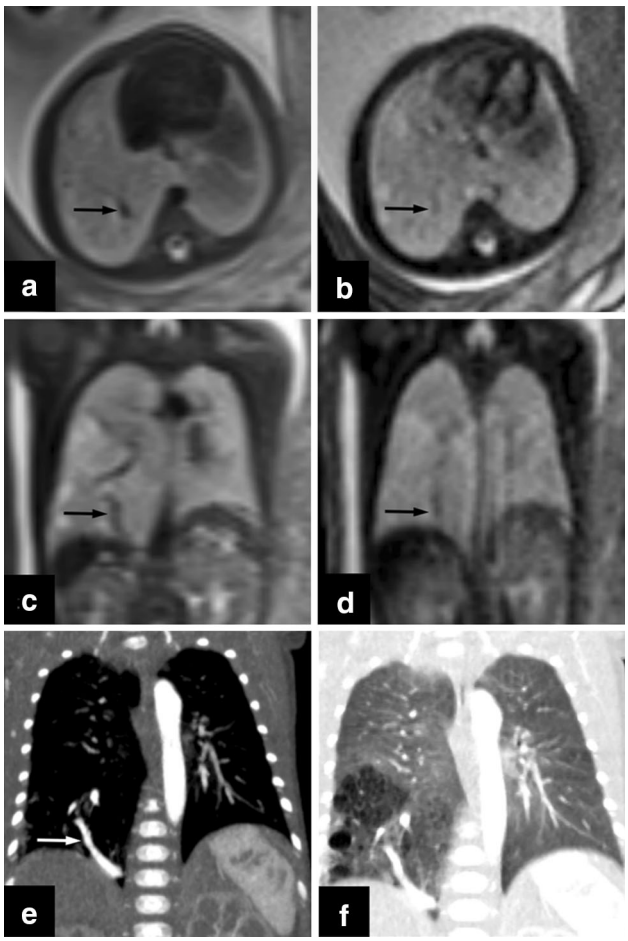

Fig. 2 ILS in the right lower lobe (Typical images representing "good" on SSTSE and "fair" on b-SSFP sequence, fetus #12). **a–d** Fetal MRI at 26 weeks' gestation (**a** SSTSE axial plane, **b** b-SSFP axial plane, **c** SSTSE coronal plane, **d** b-SSFP coronal plane). Aberrant artery is well identified on the SSTSE sequence (**a**, **c,** arrow), but is ambiguous on the b-SSFP sequence (**b**, **d,** arrow). Contrast-enhanced CT at the age of 2 days after birth reveals the aberrant artery (arrow) which shows a similar appearance to the fetal MRI (**e**, **f**)

b-SSFP sequences. Using a paired *t* test, the diagnostic power of the images on SSTSE sequences was shown to be statistically superior to those on b-SSFP sequences ($P < 0.01$ (0.0007)).

2. The relationship between the diagnostic power of the images and arterial diameter

The mean diameter of all aberrant arteries was 2.47 ± 0.72 mm (mean ± SD, range 1.2–3.7 mm). All 15 aberrant arteries were well visualized on SSTSE sequences, regardless of the diameter. On b-SSFP sequences, the mean arterial diameter of the seven fetuses with "fair" visualization was 2.3 mm, and that of the eight fetuses with "poor" visualization was 2.6 mm. There was no statistical relationship between arterial diameter and the diagnostic power of images ($P = 0.27 > 0.05$, using a Fisher's exact test).

3. The visualization of the aberrant artery in BPS and hybrid lesions

There were five BPS (fetuses #1, 3, 6, 11, and 15) and 10 hybrid lesions (fetuses #2, 4, 5, 7–10, and 12–14). The SSTSE sequence clearly demonstrated the presence of aberrant arteries in all 15 fetuses, regardless of the pathology. On b-SSFP sequence, the mean Likert scale value of the five BPS was 1.4 (three 'poor' (fetuses #1, 6, and 15) and two 'fair' visualizations (fetuses #3 and 11) were included), and that of the ten hybrid lesions was 1.5 (five 'poor' (fetuses #4, 8, 9, 13, and 14) and five 'fair' visualization (fetuses #2, 5, 7, 10, and 12) were included).

There was no statistical relationship between pathological subtype and the diagnostic power of images ($P = 0.37 > 0.05$, using Fisher's exact test).

Discussion

Although the best screening tool for diagnosing BPS in the prenatal period is definitely ultrasound, fetal MRI is also supportive in confirming the diagnosis and has an important role in obtaining more details such as defining the boundary with normal lung tissue and precise location. This modality can also estimate the volume and maturity of normal lung tissue, and other related abnormalities such as congenital diaphragmatic hernia [7]. For these reasons, at our institution, it is routine for obstetricians to request fetal MRI on fetuses suspected of BPS on ultrasound.

After delivery, neonatologists and pediatric surgeons plan how infants with BPS should be managed, depending on severity. Surgical resection can be opted for in symptomatic BPS, but follow-up care is often the management of choice in asymptomatic BPS. Contrast-enhanced CT is usually performed in the neonatal period at our institution, to evaluate the current condition and its surgical potential, and to determine whether surgery is required. Three-dimensional reconstructions and volume rendering of images can help surgeons to make their decisions based on better spatial resolution.

In this way, both prenatal images (not only ultrasound but also MRI) and postnatal image (contrast-enhanced CT) contribute to the planning and determination of perinatal management following discussion among clinicians from each department.

Our study confirmed that the SSTSE sequence is far superior to the b-SSFP sequence in detecting aberrant arteries. This finding might be due to the significant difference between the signal displayed by vessels acquired using SSTSE and b-SSFP sequences. SSTSE sequences reveal vessels as a dark signal due to the flow void phenomenon. In contrast, on b-SSFP sequences, vessels appear as a bright signal, in principle because flow compensation within vessels can be achieved in all three axes [10]. The signals acquired from viscera are quite different between the thorax and abdomen. Vessels in the thorax (thoracic aorta, pulmonary artery and vein) are surrounded by fetal lung. Fetal lung shows up as a bright signal on both SSTSE and b-SSFP sequences because it is filled with amniotic and alveolar fluid [8, 11]. This is entirely the opposite condition to the abdomen where vessels such as the portal vein and the mesenteric artery and mesenteric vein are adjacent to or surrounded by viscera with a dark signal (Fig. 3a–d). The b-SSFP sequence is a widely used technique for evaluation of cardiac and abdominal vessel

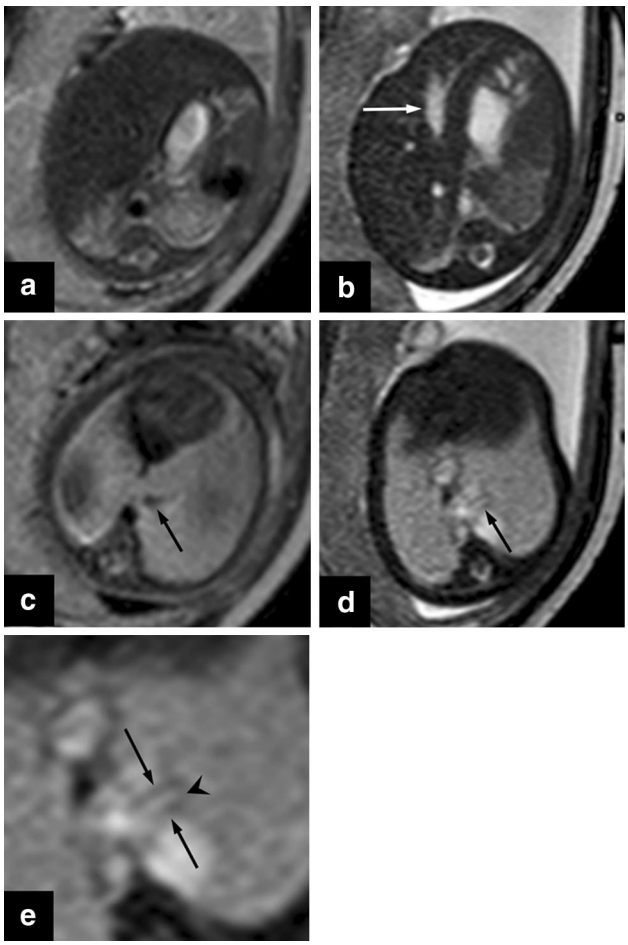

Fig. 3 Fetal MRI at 29 weeks' gestation (fetus #2): axial plane on SSTSE sequence (**a**, **c**) and b-SSFP sequence (**b**, **d**). Vessels in the liver (**b**, arrow) are well visualized on the b-SSFP sequence compared with the SSTSE sequence (**a**). In contrast, better visualization contrast between dark vessels and the bright lung can be obtained on the SSTSE sequence than on the b-SSFP sequence (**c**, **d**, arrow). In the magnified image of the b-SSFP sequence (**e**), triple lines along the aberrant artery were recognized, consisting of two dark lines (arrows) and one bright line (arrowhead)

imaging because it can provide good contrast between vessels (bright) and solid tissue (dark) [9]. The SSTSE sequence is however essential for evaluation of aberrant arteries (dark) within fetal lung (bright) in diagnosing BPS on fetal MRI. We should evaluate target vessels using the correct sequence, according to the intensity of the adjacent or surrounding tissues.

The visualization of an aberrant artery on b-SSFP was incomplete throughout the present study. Seven fetuses (46.7%) demonstrated an ambiguous appearance, and in the other eight (53.3%) the vessel was not well visualized. We initially hypothesized that the cause of the difference between "fair" and "poor" visualization on b-SSFP sequences might be differences in aberrant arterial diameter, but our results did not verify a statistically significant

relationship ($P = 0.27$), under the limitation that the number of patients was small. This result might be explained by another interpretation—that dark linear structures seen on b-SSFP sequences cannot be vessel lumens but may represent interfaces between vessel lumens and surrounding lung tissue. It is clear that in the present study, two fetuses (#2 and 11) showed triple lines (dark-bright-dark) along the course of aberrant arteries on a b-SSFP sequence (Fig. 3e). The triple lines might represent the very thin vessel wall (dark) and the lumen containing the flowing blood (bright).

The appearance of CPAM on fetal MRI depends on the size of the cysts [1]. Similarly, hybrid lesions comprising BPS and CPAM can present with a heterogeneous or mosaic-pattern appearance of various degrees on fetal MRI. We also hypothesized that the heterogeneity of a hybrid lesion might affect identification of the aberrant artery. Our ten hybrid lesions that were classified pathologically actually had a more heterogeneous appearance of varying degree on fetal MRI than was the case with BPS. From our results, we were able to assess both hypotheses. First, an SSTSE sequence can demonstrate aberrant arteries regardless of the heterogeneity of the background. Second, differences in arterial visualization on b-SSFP sequences (fetuses with 7 'fair' and 8 'poor' visualizations were included) do not depend on the background heterogeneity. Regarding the identification of the aberrant artery, there was no correlation between the diagnostic power and the pathological findings ($P = 0.37$).

Our current research has some limitations. First, our study included a fairly small number of fetuses (just fifteen); additional investigation will be needed in a larger number of fetuses. Second, our results support to the hypothesis that the diameter of an aberrant artery does not contribute to its visualization on a b-SSFP sequence, but this speculation is itself limited because the measurement of arterial diameter was done apart from the fetal MRI, with a wide range of intervals (from 1 to 54 days after birth). Spontaneous regression of sequestration and the aberrant artery might occur during the natural course of the condition. Finally, there is bias due to the retrospective nature of the study. Two reviewers simply reconfirmed the aberrant artery on fetal MRI, after referring to the postnatal, contrast-enhanced CT. Prospective evaluation can be expected to confirm the accuracy of the utility of the SSTSE sequence in diagnosing an aberrant artery.

Conclusion

The SSTSE sequence is essential for detecting aberrant arteries in the diagnosis of BPS on fetal MRI. Accuracy may not be affected by either arterial diameter or background heterogeneity.

Acknowledgements This article was supported by a Grant from the National Center for Child Health and Development, Japan, 26-20. We thank Hiroshi Nagamatsu (principal technologist), Rumi Imai, Chiharu Hiramatsu, Tomoyuki Maruyama, Keisuke Asano, and Taizo Somemori as MRI technologists of the National Center for Child Health and Development.

Compliance with Ethical Standards

Conflict of interest The authors declare that they have no conflict of interest.

References

1. Woodward PJ. Chest. In: Woodward PJ, Kennedy A, Sohaey R, editors. Diagnostic imaging: obstetrics. 3rd ed. Salt Lake City: Amirsys; 2016. p. 336–43.
2. Recio Rodriquez M, Martinez de Vega V, Cano Alonso R, Carrascoso Arranz J, Martinez Ten P, Perez Pedregosa J. MR imaging of thoracic abnormalities in the fetus. Radiographics. 2012;32:E305–21.
3. Carter R. Pulmonary sequestration. Ann Thorac Surg. 1969;7:68–88.
4. Takahashi M, Ohno M, Mihara K, Matsuura K, Sumiyoshi A. Intralobar pulmonary sequestration; with special emphasis on bronchial communication. Radiology. 1975;114:543–9.
5. Wei Y, Li F. Pulmonary sequestration: a retrospective analysis of 2625 cases in China. Eur J Cardiothorac Surg. 2011;40:e39–42.
6. Long Q, Zha Y, Yang Z. Evaluation of pulmonary sequestration with multidetector computed tomography angiography in a select cohort of patients: a retrospective study. Clinics (Sao Paulo). 2016;71:392–8.
7. Mon RA, Johnson KN, Ladino-Torres M, Heider A, Mychaliska GB, Treadwell MC, et al. Diagnostic accuracy of imaging studies in congenital lung malformations. Arch Dis Child Fetal Neonatal Ed. 2019;104:F372-7.
8. Saleem SN. Fetal MRI: an approach to practice: a review. J Adv Res. 2014;5:507–23.
9. Chavhan GB, Babyn PS, Jankharia BG, Cheng HL, Shroff MM. Steady-state MR imaging sequences: physics, classification, and clinical applications. Radiographics. 2008;28:1147–60.
10. Scheffler K, Lehnhardt S. Principles and applications of balanced SSFP techniques. Eur Radiol. 2003;13:2409–18.
11. Liu YP, Lin YL, Chen SC. Fetal magnetic resonance imaging of congenital chest malformations: a pictorial review. J Radiol Sci. 2013;38:119–27.